

See discussions, stats, and author profiles for this publication at: <https://www.researchgate.net/publication/336648656>

# Automotive Radar Sensor Behavioral Models for Closed Loop Simulations

Preprint · October 2019

CITATIONS

0

READS

163

8 authors, including:



**Arsalan Haider**

Hochschule für angewandte Wissenschaften Kempten

8 PUBLICATIONS 20 CITATIONS

SEE PROFILE



**Marcel Sachse**

Hochschule für angewandte Wissenschaften Kempten

2 PUBLICATIONS 1 CITATION

SEE PROFILE



**Thomas Zeh**

Technische Universität München

24 PUBLICATIONS 84 CITATIONS

SEE PROFILE



**Stefan-Alexander Schneider**

Hochschule für angewandte Wissenschaften Kempten

175 PUBLICATIONS 122 CITATIONS

SEE PROFILE

Some of the authors of this publication are also working on these related projects:



ADAS Sensor Modeling [View project](#)



CLOVER - Robust Control, State Estimation and Disturbance Compensation for Highly Dynamic Environmental Mechatronic Systems [View project](#)

# Automotive Radar Sensor Behavioral Models for Closed Loop Simulations

Arsalan Haider, Jihoon Kim, Marcel Sachse, Thomas Zeh, Stefan Alexander Schneider,  
Matthias Thumann, Abdulkadir Eryildirim and Tim Ebeling

*University of Applied Sciences, Kempten*

*Bahnhofstraße 61 Kempten, Bavaria, 87435, Germany*

*arsalan.haider@hs-kempten.de*

*jihoon.kim@stud.hs-kempten.de*

*marcel.o.sachse@stud.hs-kempten.de*

*thomas.zeh@hs-kempten.de*

*stefan-alexander.schneider@hs-kempten.de*

*matthias.thumann@stud.hs-kempten.de*

*Abduelkadir.Eryildirim@infineon.com*

*tim.ebeling@stud.hs-kempten.de*

September 13, 2019

**Keyword(s):** ADAS, FMU, OSI, FMCW, radar behavioral model, FMI,  
HAD Function, FFT, CarMaker, AEB

## Abstract

The goal of the presented work is to develop an automotive radar sensor behavioral model to outline closed loop interaction of driver and vehicle in a synthetic environment. For this interaction open simulation interface (**OSI**) and functional mock-up interface (**FMI**) standards are used. This paper describes the architecture overview, working concept of FMI, OSI and different radar functions like radar channel and digital signal processing (**DSP**) in detail. The description of the scenario for the verification of radar behavioral model results and development of highly automated driving (**HAD**) functions for the closed loop simulation is elaborated in this paper.

## I. Introduction

The development and validation of suitable radar sensors is in the focus of advanced driver assistance systems (**ADAS**) and autonomous driving (**AD**). The behavior of HAD functions heavily depends on the detected and classified objects and with that on the detection and the classification quality of the corresponding sensor data. In automotive applications, frequency modulated continuous wave (**FMCW**) radar sensors play an important role. To cope with the enormous amount of validation efforts, modern simulation methods need to be introduced. The required resolution of the system simulation of driver, vehicle and environment depends on the actual HAD functions, e.g. an autonomous emergency break (**AEB**) needs high resolution of the area of the most probable path of the vehicle whereas, a parking assistant (**PA**) needs an overall environmental resolution as given in Fig.1. This need of different levels of abstractions for the components of the system requires a well-structured architecture of the system and its interfaces modelling. This is especially true for the interface, between the vehicle and environment. The accuracy depends on the scenarios, the resolution of the components and their joint simulation. This validation is a topic for its own. Here, it is advisable to perform both components as well as system tests, keeping all these aspects in mind, we propose the architecture of a radar sensor behavioral model as given in Fig. 2 and Fig. 3 respectively.

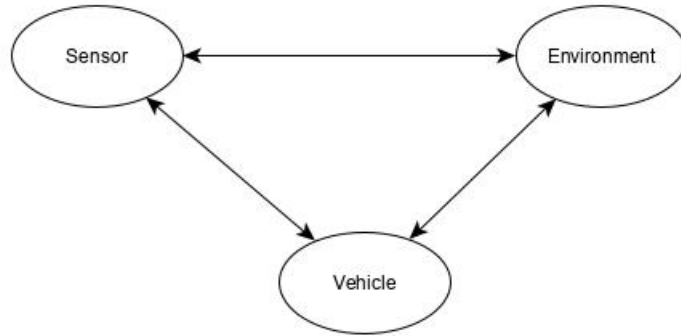


Figure 1: Interaction of control loop of autonomous driving

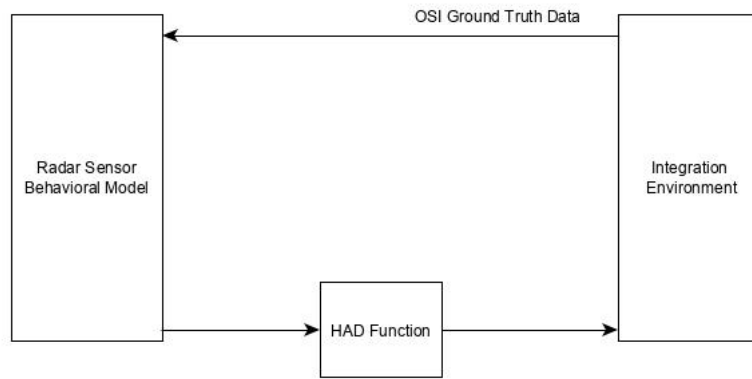


Figure 2: Closed loop Block diagram of an FMCW radar FMU with **IF** sampling methodology

## II. Architecture overview of Radar Behavioral Model

The proposed radar sensor behavioral model consists of the following overall four components: Integration Environment, Radar Channel, DSP and HAD function. The interfaces of the components are implemented in system according to the FMI 2.0 standard. Only the interaction between the components Radar Channel and Environment needs the extension of OSI. Therefore all components are implemented as functional mock-up unit (**FMU**) or so called OSI FMUs. This architecture allows an integration of different inputs from original equipment manufacturer (**OEM**) and suppliers to perform a closed loop simulation for development and validation purposes. In this paper, we focus to establish a low maintainable system simulation. In this paper, we use as authoring tools for the FMUs, the programming languages C/C++, CMake, Visual Studio 2017, Protocol Buffers and CarMaker as integration platform in version 6.0.6 from the company IPG Automotive providing OSI in version 2.2 support.

## III. Functional Mock-up Interface

FMI is an answer to the industrial need to exchange models between different tools. This occurs i.g for modelling and simulation purpose or for the system design. FMI supplies this possibility via defined interfaces [1]. FMI defines a C interface that is implemented by an executable called a FMU. As illustrated in Fig. 4, it is possible to connect the commercial simulation software with the independent "Sensor Behavioral Model" via FMI.

## IV. Open Simulation Interface

The main goal behind the development of OSI is being able to connect any (automated driving function) to any (driving) simulator with ease. To enable easy and straight forward compatibility between automated driving functions and the variety of driving simulation frameworks available, the OSI standard can be used. This will simplify the integration and therefore significantly strengthen accessibility and usefulness of virtual testing. For

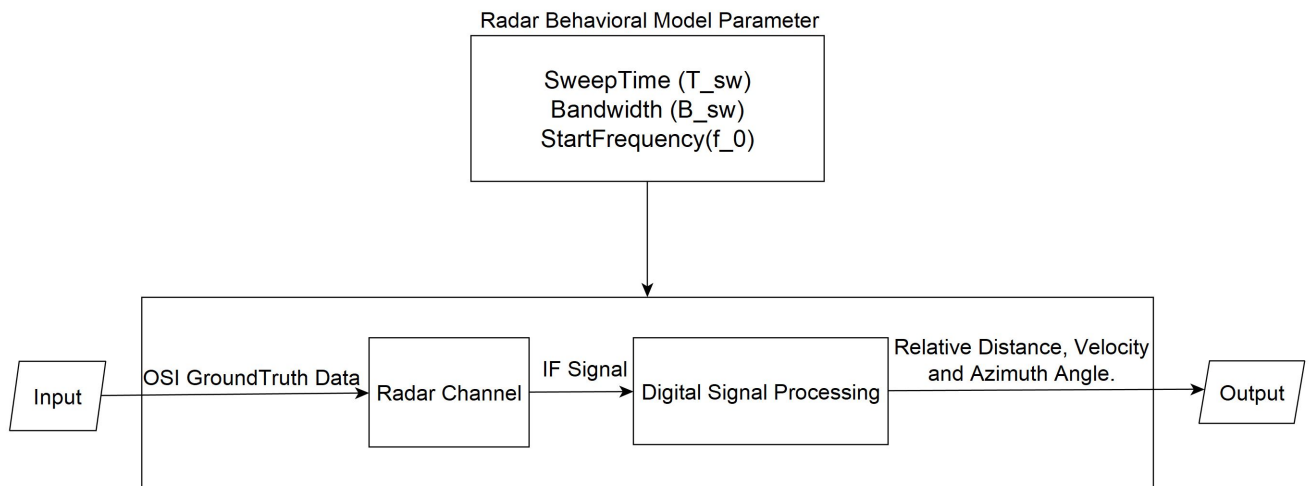


Figure 3: Block diagram of an FMCW radar FMU with **IF** sampling approach

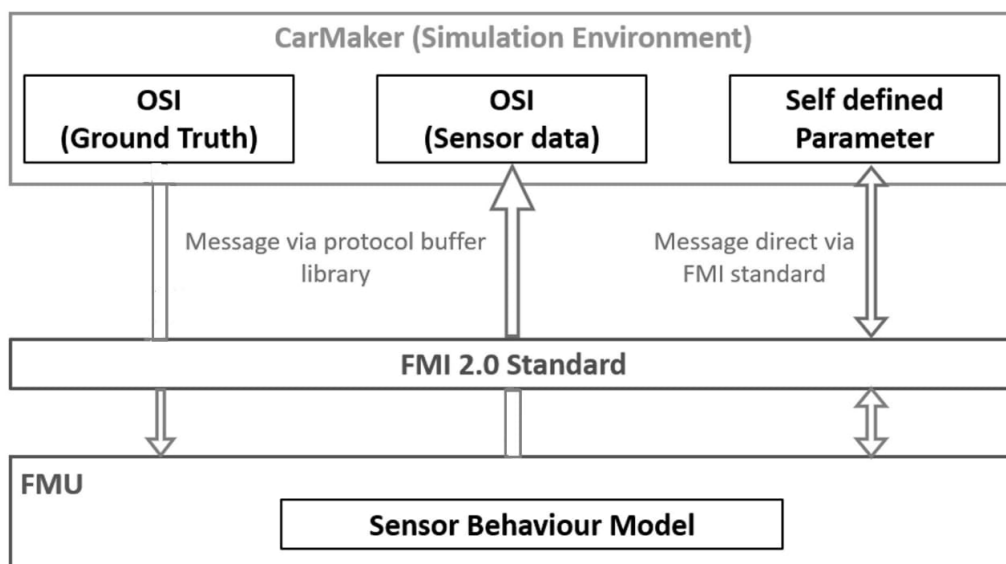


Figure 4: General concept of the Radar Behavioral Model

the circumstance of this work, OSI is needed to detect, the current position of the ego car, radar sensor, velocity and orientation of the traffic car. With these informations an object reflected signal can be calculated that is necessary for the further data processing inside the radar as explained in section V. To use the OSI concept protobuf must be installed (for this work protobuf version 2.6.1) on the system. Fig. 5 shows an example how the required information like dimension, position, velocity or orientation of a car in reference to the global coordinate system can be accessed. The function argument `{veh}` contains all information about a vehicle from the simulation environment.

```
void CRadarModel::VehicleParameter(double &length, double &width, double &height, const osi::Vehicle veh)
{
    length = veh.base().dimension().length();
    width = veh.base().dimension().width();
    height = veh.base().dimension().height();
}
```

Figure 5: Access to different OSI variables. Example of the `{osi::Vehicle}` structure

## V. Implementation strategy of a FMCW Radar behavioral model

There are two different approaches possible for the implementation of the Radar Behavioral Model. The radio frequency (**RF**) and the intermediate frequency (**IF**) approach. This work focus on IF approach because it requires much less memory and computation time as compared to RF. In this approach signal generator and mixer is not required and the IF signal is generated in Radar Channel. The value of IF sampling rate,  $f_{sIF}$  is determined by the maximum target range to be considered. The IF sampling frequency can be given as

$$R_{max} = \frac{c \cdot T_{sw} \cdot f_{sIF}}{2 \cdot B_{sw} \cdot 2} \quad (1)$$

$$f_{sIF} = \frac{4 \cdot B_{sw} \cdot R_{max}}{c \cdot T_{sw}} \quad (2)$$

where

Symbols	Meaning	Units
$R_{max}$	Maximum target range	[m]
$[\frac{B_{sw}}{T_{sw}}] \kappa$	Slope of ramp	$[\frac{1}{s^{-2}}]$
$B_{sw}$	Bandwidth	[Hz]
$T_{sw}$	The sweep duration of ramp	[s]
$f_{sIF}$	The IF sampling frequency	[Hz]
$c$	The speed of light	[Hz]

Table 1:  $f_{sIF}$  equation parameters

## VI. Radar Channel

Radar Channel is one of the most important component of a real radar sensor and also of the radar behavioral model. The GroundTruth data from the virtual scenario of CarMaker is obtained in this section via OSI. The time delay between the transmitted and received electromagnetic waves is calculated by using the given below equation [15].

$$\Delta t = \frac{2 \cdot R}{c} \quad (3)$$

where

Symbols	Meaning	Units
$R$	The range of the object in virtual scenario	[m]
$c$	The speed of light	[m/s]
$\Delta t$	The time delay	[s]

Table 2:  $\Delta t$  equation parameters

The Doppler frequency is calculated by the following equation [15]

$$f_D = \frac{2 \cdot f_0 \cdot v_r}{c} \quad (4)$$

where

The radial velocity and range of objects are found by using the equations [15]

$$R_{GT} = \frac{c \cdot \Delta t}{2} \quad (5)$$

$$v_{rGT} = \frac{c}{2 \cdot f_0} \cdot f_D \quad (6)$$

Symbols	Meaning	Units
$f_D$	The Doppler frequency	Hz]
$c$	The radar transmission frequency	[Hz]
$f_0$	The time delay	[s]
$v_r$	The relative speed of the object	[m/s]

Table 3:  $f_D$  equation parameters

In the case when, the sending and transmitting antennas of a automotive radar are at the same place it is referred as a Mono-static radar. The classic radar equation is used for free space loss as given below [15]

$$P_r = \frac{P_t \cdot G_t \cdot G_r \cdot \lambda^2 \cdot \sigma}{(4\pi)^3 R^4} \quad (7)$$

where

Symbols	Meaning	Units
$P_t$	Transmission power	[W]
$P_r$	Receiving power	[W]
$G_t$	Gain of transmission antenna	[dB]
$G_r$	Gain of received antenna	[dB]
$\lambda$	The wavelength $\frac{c}{f}$	[m]
$\sigma$	Radar cross section (RCS)	[m <sup>2</sup> ]
$R$	The distance between radar and target	[m]

Table 4:  $P_r$  equation parameters

The object amplitude is calculated by using

$$A_{RX} = \sqrt{P_r \cdot 2 \cdot R_{antenna}} \quad (8)$$

where

Symbols	Meaning	Units
$A_{RX}$	Amplitude of RX antenna	[V]
$P_r$	Receiving power of antenna	[W]
$R_{antenna}$	Resistance of antenna	[ $\Omega$ ]

Table 5:  $A_{RX}$  equation parameters

$$A_{TX} = \sqrt{P_t \cdot 2 \cdot R_{antenna}} \quad (9)$$

where

Symbols	Meaning	Units
$A_{TX}$	Amplitude of TX antenna	[V]
$P_t$	Transmitting power of antenna	[W]
$R_{antenna}$	Resistance of antenna	[ $\Omega$ ]

Table 6:  $A_{TX}$  equation parameters

$$A_{IF} = A_{TX} \cdot A_{RX} \quad (10)$$

where

Symbols	Meaning	Units
$A_{IF}$	Amplitude of IF signal	[V]

Table 7:  $A_{IF}$  equation parameters

#### A. Virtual Antenna Array

In order to calculate the azimuth angle a multiple input – multiple output (**MIMO**) antenna array concept is used in this work without any orthogonality by considering that antennas can transmit and receive the signals simultaneously. In this case, a very simple type of isotropic antenna is considered with only one main lobe. The static gain is considered for TX and RX antennas without any loss. The spacing between the receiver antennas is  $d = \lambda/2$  and between transmitting antennas is  $4d$  as given in Fig. 6.

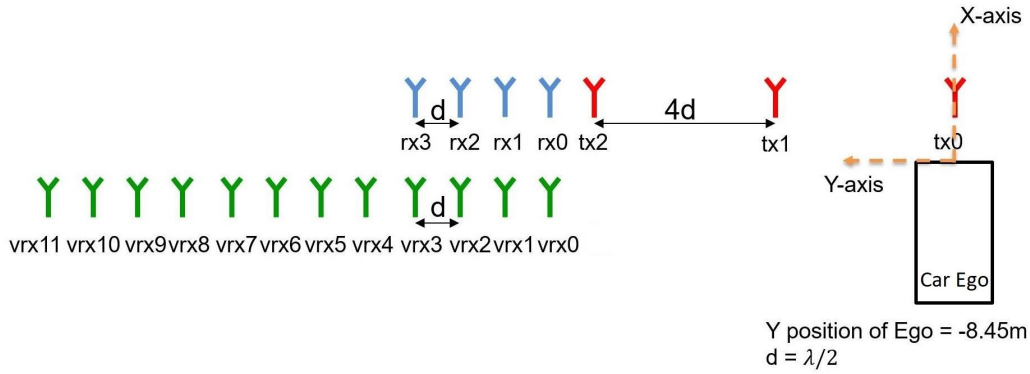


Figure 6: Implemented virtual antenna array

#### B. Intermediate Frequency Signal Generation

The parameters calculated in radar channel are used to generate the IF signal model [16].

$$S_{IF}(t) = A_{IF} \cos(2\pi\kappa t\tau + 2\pi f_{start}\tau - \pi\kappa\tau^2) + noise \quad (11)$$

In this research work additive white Gaussian noise (**AWGN**) is considered which means a zero-mean normal distributed signal with ( $\mu = 0$ ) and unity variance ( $\sigma^2 = 1$ ) is added to the IF signal.

Parameters	Value	Units
No. of TX	3	[1]
No. of RX	4	[1]
Static gain for TX and RX	12	[dB]
field of view (FOV)	$-90^\circ$ to $+90^\circ$	[ $^\circ$ ]
Number of channels	12	[1]

Table 8: Parameter of virtual antenna array

Symbols	Meaning	Units
$\kappa = \frac{B_{sw}}{T_{sw}}$	Slope of ramp	[Hz/s]
$\tau_o = \frac{2 \cdot R}{c}$	Round trip delay time	[s]
$\tau = \tau_o + \frac{v_r(nT_{sw} + t)}{c}$	Additive White Gaussian Noise	[V]

Table 9: Parameter of  $S_{IF}$

## VII. Digital signal processing

### A. Generation of Range Doppler Matrix

The information about the time delay (range) and Doppler shift (due to movement) of the radar targets are determined by the double two-dimensional discrete fast Fourier transform (**DFT**) technique [18]. The detail working of double two-dimensional DFT technique can be found in [19]. In this work, the first FFT is carried out over a samples of each  $k^{th}$  sweeps to determine the time delay spread over range bins and second FFT is applied on the number of sweeps at each  $m^{th}$  time delay bin to obtain the Doppler information [18]. In other words, the input of second FFT is the range bins output of first FFT. So, in this work the second FFT is carried over 128 sweeps at each 512 range bins to obtain the Doppler information [18].

Before applying the FFT Hanning window or Rectangular window is applied in order to reshape the IF signal and obtain the information about the weak targets [20].

$$W_{hn}[n] = 0.5[1 - \cos(2\pi n/N - 1)] \quad 0 \leq n \leq N - 1 \quad (12)$$

Mathematical model of Rectangular window can be given as [20]

$$W_r[n] = \begin{cases} 1, & 0 \leq n \leq N - 1 \\ 0, & \text{otherwise} \end{cases} \quad (13)$$

Parameters	Value	Units
No. of Ramps	128	[1]
1D FFT points	Rectangular window 1024	[1]
2D FFT points	Rectangular window and 128 points	[1]
3D FFT points	1024 Zero padding	[1]

Table 10: Parameters for range Doppler matrix

### B. Non-Coherent Integration

In order to improve the detection process, the data of multiple receiving channel can be used although the detection take place before the angular processing [21]. The complex values of each channel are summed up in order to calculate the square magnitude. The summation of complex values of several channels signals can interfere, either constructively or destructively [21]. In such a case non-coherent integration (**NCI**) is required in

power spectrum to avoid cancellation of signal power. As already given in section VI (subsection B) that AWGN is used to model real and imaginary components of noise. Which, will follow zero-mean normal distribution in frequency domain [21]. By the summation of complex squared values, the power spectrum can be calculated. As given in [21] two squared values sum, those are independent and identically distributed Gaussian variables, results in chi-squared distribution  $\chi^2(n)$  having ( $n = 2$ ) two degree of freedom.

$$|N[k]|^2 = N_{RE}[k]^2 + N_{im}[k]^2$$

$$|N[k]|^2 \sim \chi^2(2)$$

But the sum of multiple receiving channels, independent and identically distributed Gaussian variables, will result in chi-squared distribution again but with high degree of freedom [21]. NCI is required when there is phase mismatch between the signals of adjacent channels owing to receiver phase drift, Doppler frequency ambiguity and miscellaneous data [22].

### C. Cell-Averaging Constant False Alarm Rate

In this work, a very simple Cell-Averaging constant false alarm rate (**CA-CFAR**) scheme is used. The main reason behind the use of this scheme to calculate adaptive threshold level by approximating the noise level around the cell under test (**CUT**). This adaptive threshold level help to determine is the cell under test (**CUT**) have target inside it or only unwanted false alarm. The detail working of CA-CFAR can be found in [21,23]. Fig. 5 depict the implemented CA-CFAR flow chart in this work.

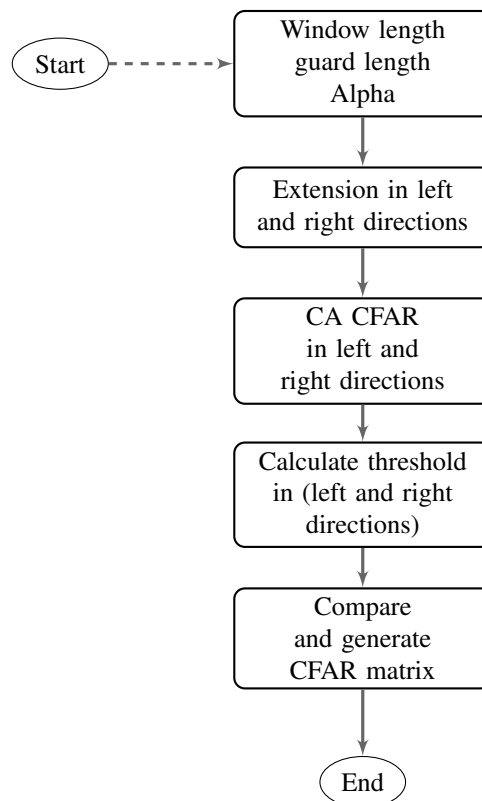


Figure 7: CA-CFAR Flow Chart

### D. Angle Estimation

Mechanical steered antenna and virtual antenna array can be used for the azimuth angle estimation ( $\theta_e$ ) as given in [21]. But in this work virtual antenna array concept is used for the angle estimation as given in subsection A.

Parameter	Value	Units
Window length	10	[1]
Guard length	8	[1]
Alpha	10	[1]

Table 11: Parameter of CA-CFAR

In this method, every time delayed version of transmit signal is fed to each antenna element as depicted in Fig. 6. In order to determine the direction of arrival (**DOA**), 3D FFT is applied on the peak values of 2D Range Doppler Matrix corresponding to every virtual antenna array elements. The detail working of angle estimation can be found in [21,24].

### VIII. Specification for the verification of Radar behavioral model results

There are three outputs of this radar behavioral model, i.e distance, velocity and the orientation in azimuth angle. The goal of this model only to have estimated<sup>1</sup> distance, velocity and azimuth angle values in their resolution. The verification of this model results are done on the base of plausibilisation and in future test bed will be developed in order to verify the results further. The specifications of the model are given in Table 12.

Parameter	Value	Units
Ramp Sweep duration	40	[ $\mu$ s]
Bandwidth	1	[GHz]
Number of Ramps	128 per channel	[1]

Table 12: Specification of radar behavioral model

The maximum detectable distance of this radar behavioral model can be given as

$$R_{max} = \frac{c \cdot f_{SIF}}{4 \cdot \kappa} = \frac{2.99792458 \cdot 10^8 \cdot 25 \cdot 10^6 \cdot 40 \cdot 10^{-6}}{4 \cdot 1.0 \cdot 10^9} = 75 \text{ [m]} \quad (14)$$

The maximum detectable velocity can be given as

$$v_{max} = \frac{c}{4 \cdot f_0 \cdot T_{sw}} = \frac{2.99792458 \cdot 10^8}{4 \cdot 77 \cdot 10^9 \cdot 40 \cdot 10^{-6}} = 24 \text{ [m/s]} \quad (15)$$

The range and velocity resolutions are given below respectively,

$$\text{Range Resolution} = \frac{c}{2 \cdot B_{sw}} = \frac{2.99792458 \cdot 10^8}{2 \cdot 1.0 \cdot 10^9} = 0.15 \text{ [m]} \quad (16)$$

$$\text{Velocity Resolution} = \frac{c}{4 \cdot N_m \cdot T_{sw} \cdot f_s} = \frac{2.99792458 \cdot 10^8}{4 \cdot 128 \cdot 40 \cdot 10^{-6} \cdot 77 \cdot 10^9} = 0.19 \text{ [ms}^{-1}\text{]} \quad (17)$$

$$\text{Angle Resolution} = \frac{2}{N} = \frac{2}{12} = 0.16666\text{grad} \quad (18)$$

<sup>1</sup>Estimate term use for calculated results by Radar Behavioral Model.

$$\text{Angle Resolution} = 0.16666 \cdot \frac{180^\circ}{\pi} = 9.5^\circ \quad (19)$$

## IX. Scenario Description

### A. Test Environment

In order to test the radar behavioral model, a simulation scenario is generated in CarMaker software version 6.0.6. The test takes place on a two-lane highway with service lane. The road is straight and 10 [km] long. The driving lane left and right has a width of 3.5 [m]. The road boarder left, and right is 1 [m] wide. The lane is limited by crash barriers on the left side of the fast lane and on the right side of the service lane. The speed limit is set to 120 [kmh<sup>-1</sup>] which is indicated by road signs. The environment around the road is slightly mountainous with escarpments in form of small tree gatherings. A clear blue sky without clouds is used. An area of 0.38 [km<sup>2</sup>] around the highway is textured.

### B. Test Description

At simulation begin, ego vehicle in this example is a yellow VW Beetle model 2012 start after the beginning of the simulated highway in the fifth gear with a velocity of 100 [kmh<sup>-1</sup>] on the right side of the road. At the same time, one blue target vehicle (A1) VW Beetle start 196 [m] in front of ego vehicle and driving on fast lane. A1 is driving with 80 [kmh<sup>-1</sup>] to simulate a slowly proceeding traffic on the highway. The ego car approach this car, overtake it and continue moving until the simulation time of 60 [s] is reached which is the end condition of the simulation.



Figure 8: Objects classification in scenario

### C. HAD Function

In this paper a simple HAD function AEB is implemented. The HAD function task is to decelerate safely the vehicle to the velocity of the target vehicle ahead, see [25]. The time to collision  $t_{tc}$  with a time-threshold-brake is compared in order to decide if a braking intervention is required see [25]. The input of HAD function is relative estimated distance  $R_e$  and velocity  $v_e$  calculated by radar behavioral model and on the base of this information time-to-collision is calculated as follows see [25]:

$$t_{tc} = \frac{R_e}{v_e} \quad (20)$$

With relative distance  $R_e$  and relative velocity  $v_e$  between the ego and the target vehicle, the time threshold brake  $t_{tb}$  for a stationary target is calculated in following way [25].

$$t_{tb} = \tau_b + \frac{v_e}{2.D_{max}} \quad (21)$$

where, brake loss time  $\tau_b = 0.2$  and  $D_{max} = 6.5$  [ $\text{km s}^{-1}$ ] is considered in this case. If  $t_{tc} < t_{tb}$  then emergency brake is applied to brake the vehicle.

## X. Simulation Results and Conclusion

The simulation flow in radar behavioral model is given in Fig. 10. A very simple scenario only with single point target is generated in CarMaker in order to validate the radar behavioral model results as given in section IX. Till 21.8 [s] the target is not in the detectable range of the sensor that's why after 20 [s] sensor is not able to detect target as depict in Fig. 9. Fig. 11 depict that target is in detectable range of radar sensor but relative estimated distance  $R_e$ <sup>2</sup> is zero and velocity  $v_e = -24$  [ $\text{m s}^{-1}$ ]<sup>3</sup> as compared to virtual<sup>4</sup> GroundTruth relative distance  $R_{GT}$  and velocity  $v_{GT}$  values. The main reason behind this deviation is very low peak of signal due to the consideration of white gausain noise as given in equation 11. In the next results at 30 [s] and 36 [s] the ego vehicle approaches target more closely so reflected signals peaks are high and radar sensor estimated values of relative distance  $R_e$ , velocity  $v_e$  and angle  $\theta_e$  are approxiamtely same to the virtual GroundTruth values. After 36 [s] the ego vehicle take over the target vehicle and target is not in field of view of ego vehicle because  $\lambda/2$  spacing is considered between the receiving antennas. As already given in section VIII, the goal of this behavioral model is to have estimated values of relative distance  $R_e$ , velocity  $v_e$  and angle  $\theta_e$  in their resolution so, the results depict in Fig. 14, 15, 16, 17 validate this assumption but Fig. 18 illustrate a large deviation in azimuth angle as it approaches to  $90^\circ$ . This large deviation is due to the standard beamforming with angle FFT. Fig. 20 illustrate angle error will increase with higher angle of arrival (**AoA**) of objects because the max value occurs at the left edge of the spectrum, divided main lobe. In order to validate the performance of radar behavioral model further a simple HAD function FMU is integarted into CarMaker. In order to test the performance of HAD function a small modification is done in the scenario given in section IX. A stationary target is placed infront of ego vehicle at the distance of 200[m] and target on left line is removed as this model only can detect the single point target. Ego vehicle is moving with a speed of 80 [ $\text{km/h}$ ] as depict in Fig 25. When time to collision reaches 1.9 [s] the AEB brake is applied and speed is start reducing untill it reaches stand still as illustrate in Fig. 26 and Fig. 27 respectively.



FMU 'RadarModel': FMI: doCalc function was called..  
 FMU 'RadarModel': FMI: Not in detectable range

Figure 9: Radar behavioral model FMU output till 20 [s] of Simulation

<sup>2</sup>Distance RDM starts from 0 to 75 [m]

<sup>3</sup>Velocity RDM starts from  $-24$  [ $\text{m s}^{-1}$ ] to  $+24$  [ $\text{m s}^{-1}$ ].

<sup>4</sup>virtual term use for OSI values.

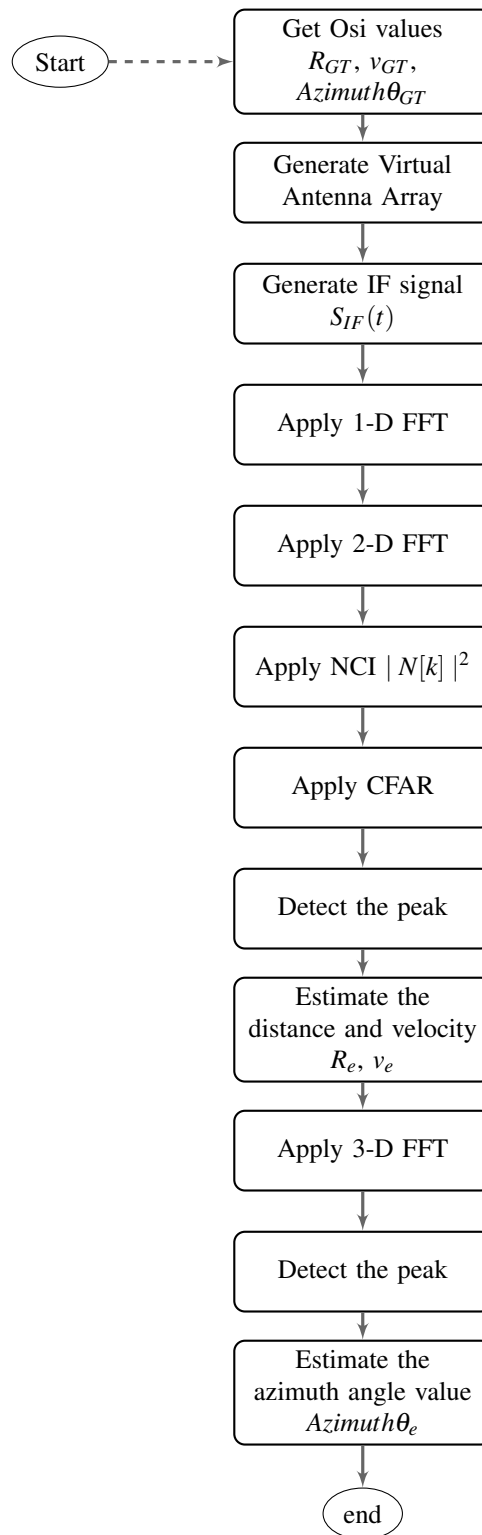


Figure 10: Simulation flow in radar behavioral model



FMU 'RadarModel': FMI: doCalc function was called..  
 FMU 'RadarModel': FMI: Estimated distance ( $R_e$ ) = 0.000000  
 FMU 'RadarModel': FMI: Virtual ground truth distance ( $R_{GT}$ ) = 73.564505

FMU 'RadarModel': FMI: Estimated velocity ( $v_e$ ) = -24.333803  
 FMU 'RadarModel': FMI: Virtual ground truth velocity ( $v_{GT}$ ) = -5.538649

FMU 'RadarModel': FMI: Estimated azimuth angle (Azimuth  $\theta_e$ ) = 90.000000  
 FMU 'RadarModel': FMI: Virtual ground truth azimuth angle (Azimuth  $\theta_{GT}$ ) = 3.039043

Figure 11: Radar behavioral model FMU output after 22 [s] of Simulation



FMU 'RadarModel': FMI: doCalc function was called..  
 FMU 'RadarModel': FMI: Estimated distance ( $R_e$ ) = 29.276607  
 FMU 'RadarModel': FMI: Virtual ground truth distance ( $R_{GT}$ ) = 29.348063

FMU 'RadarModel': FMI: Estimated velocity ( $v_e$ ) = -5.513127  
 FMU 'RadarModel': FMI: Virtual ground truth velocity ( $v_{GT}$ ) = -5.497910

FMU 'RadarModel': FMI: Estimated azimuth angle (Azimuth  $\theta_e$ ) = 7.745067  
 FMU 'RadarModel': FMI: Virtual ground truth azimuth angle (Azimuth  $\theta_{GT}$ ) = 7.637133

Figure 12: Radar behavioral model FMU output after 30 [s] of Simulation



FMU 'RadarModel': FMI: doCalc function was called..  
 FMU 'RadarModel': FMI: Not in FoV

Figure 13: Radar behavioral model FMU output after 36 [s] of Simulation

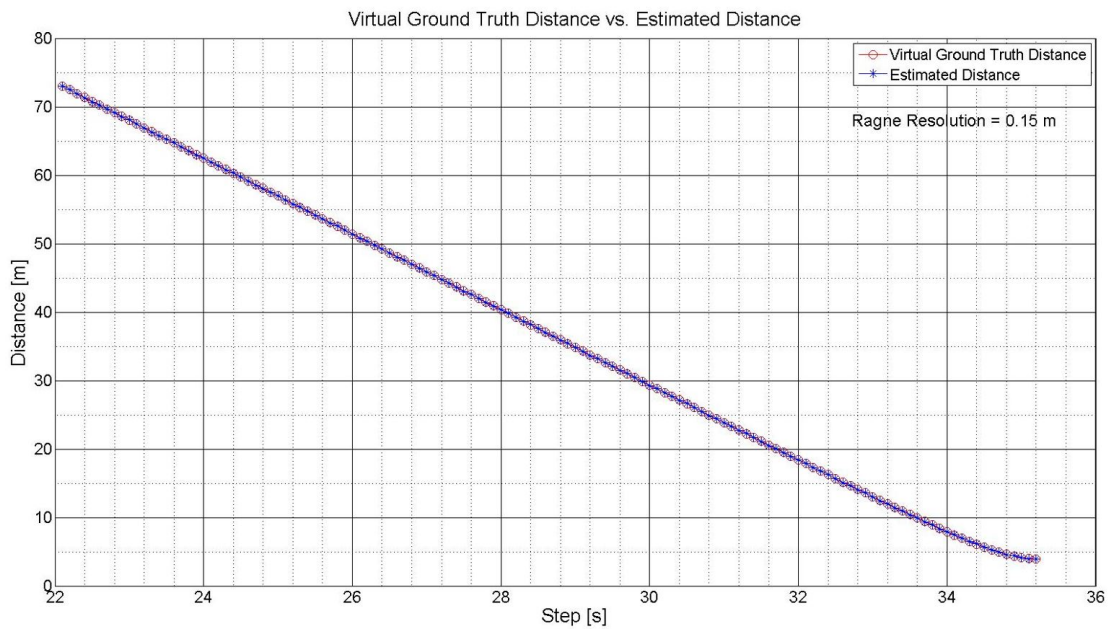


Figure 14: Virtual GroundTruth distance vs estimated distance

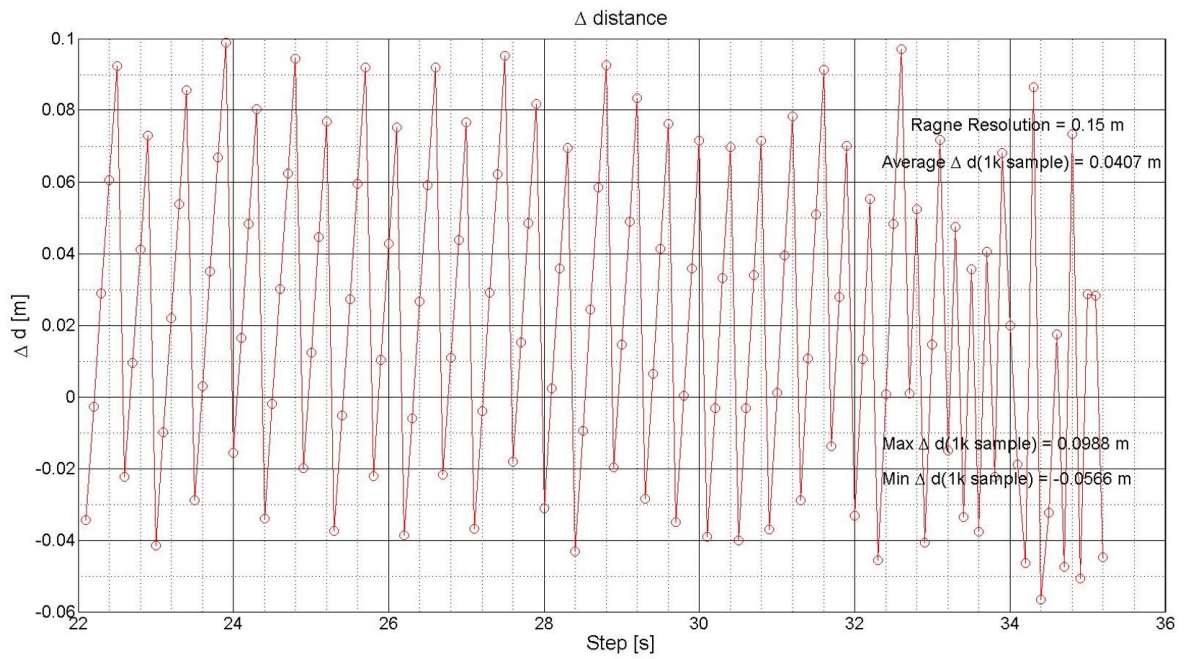


Figure 15: Delta plot of distance Values

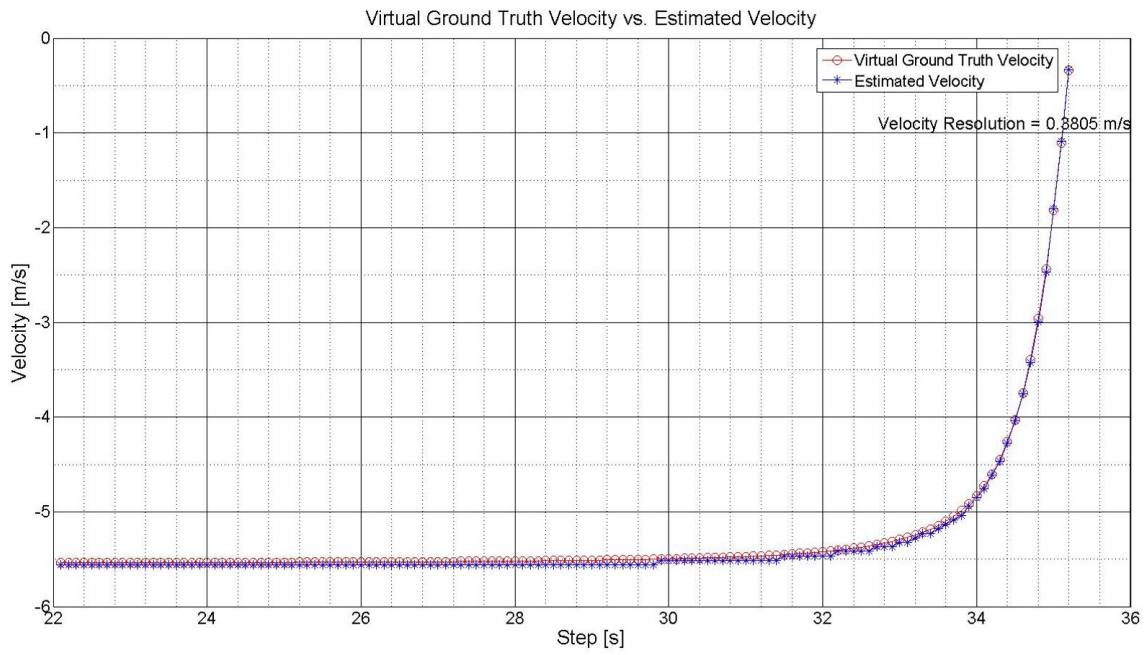


Figure 16: Virtual GroundTruth velocity vs estimated velocity

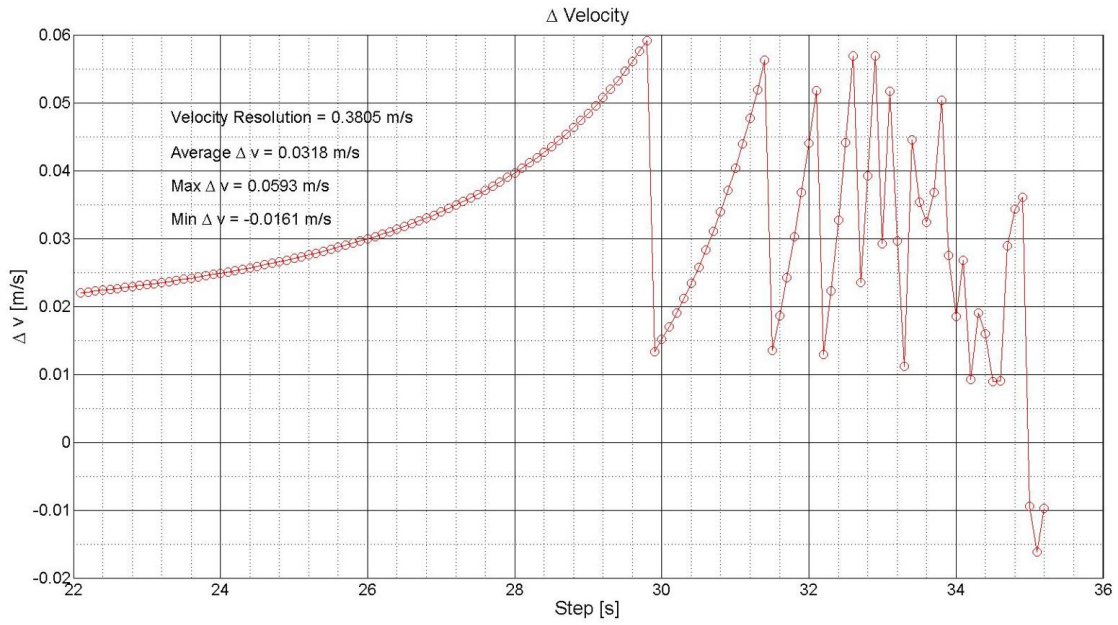


Figure 17: Delta plot of velocity values

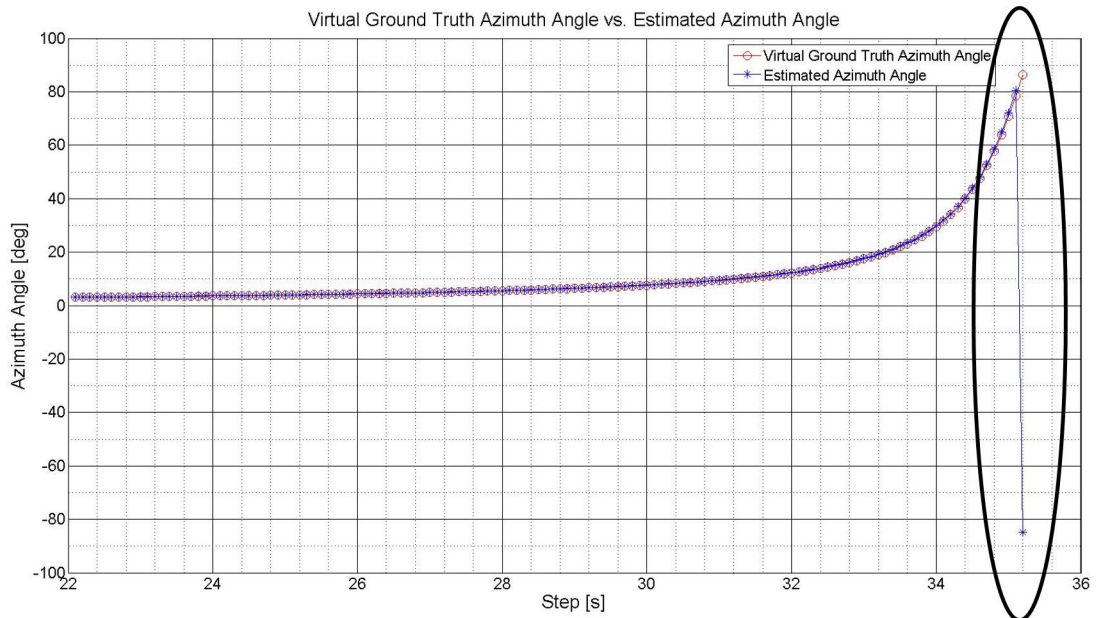


Figure 18: Virtual GroundTruth Azimuth angle vs estimated Azimuth Angle

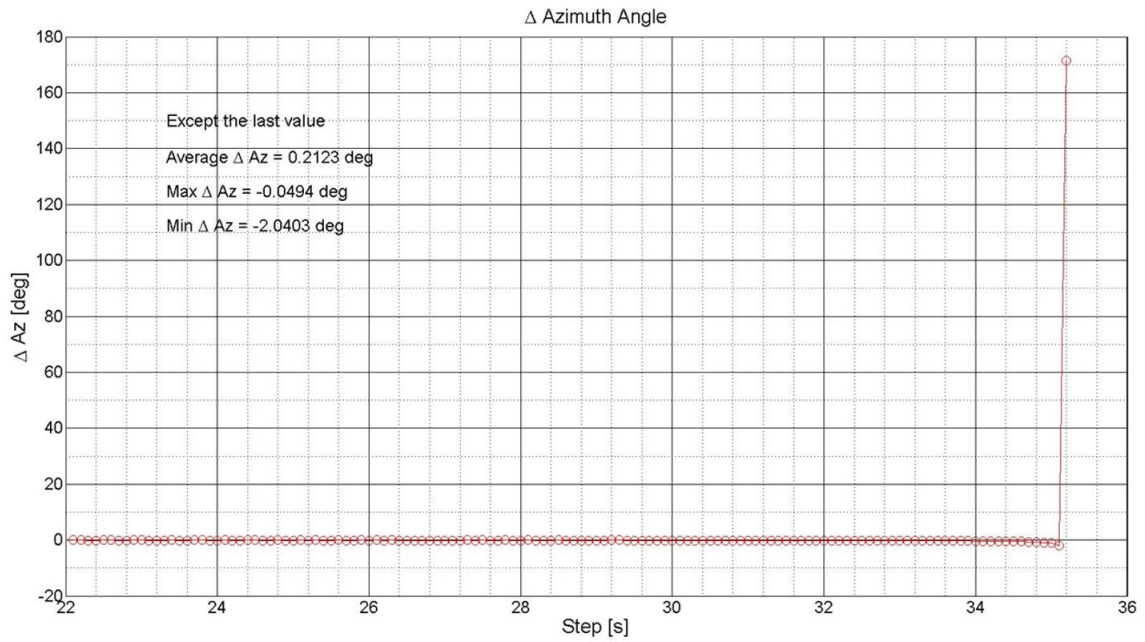


Figure 19: Delta plot of Azimuth angle

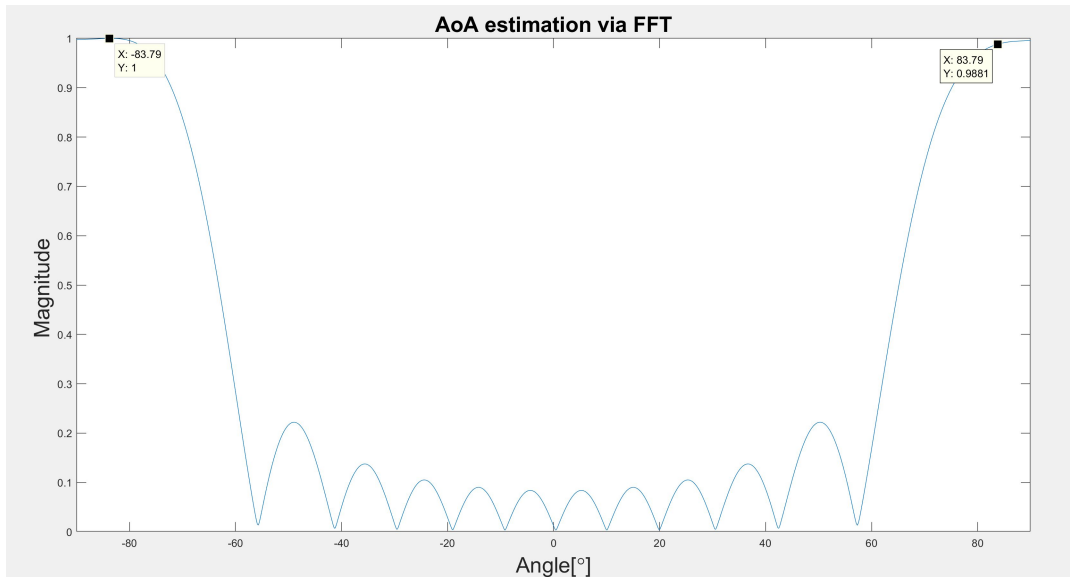


Figure 20: Deviation of Azimuth Angle

In order to investigate further the performance of radar behavioral model functions, 2D RDM (Range Doppler Matrix) is plotted for different virtual antenna channels, NCI and CFAR as given in Fig. 21, 22 and 23 respectively. In order to obtain these results a very simple scenario is generated where, the ego vehicle position in three coordinates is  $[0,0,0]$ , target position is  $[10,20,0]$ , relative velocity between the ego and target was  $[-20,0,0]$  [m/s] respectively and the angle of arrival of target was  $26.8135^\circ$ . In the Fig. 21 and 22 rectangular lines are appearing indicating the relative range and velocity values of target and also the side lobes of Hanning window. Here it is advisable to note Digital Beamforming leads to an estimation of  $(-\sin \theta)$  so in order to make the angle positive it may be applied with  $(-1)$  or need to take the inverse of vector that has the peak values of all 12 channels of 2-D RDM and needs to apply 3D FFT on it.

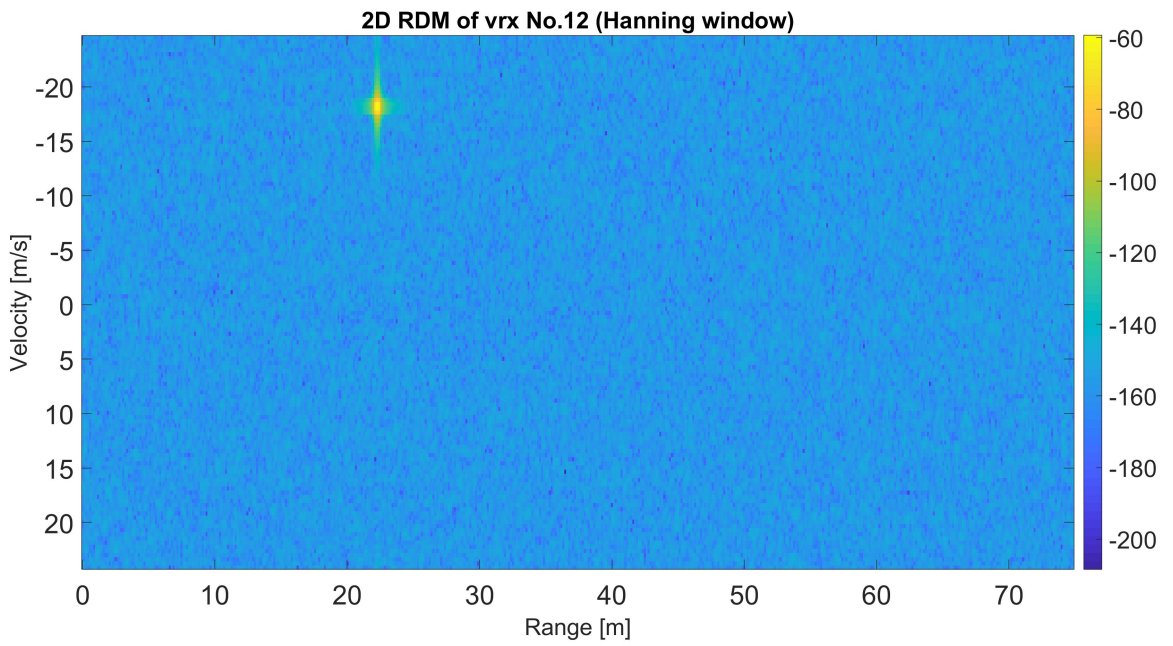


Figure 21: 2D RDM of virtual channel 12

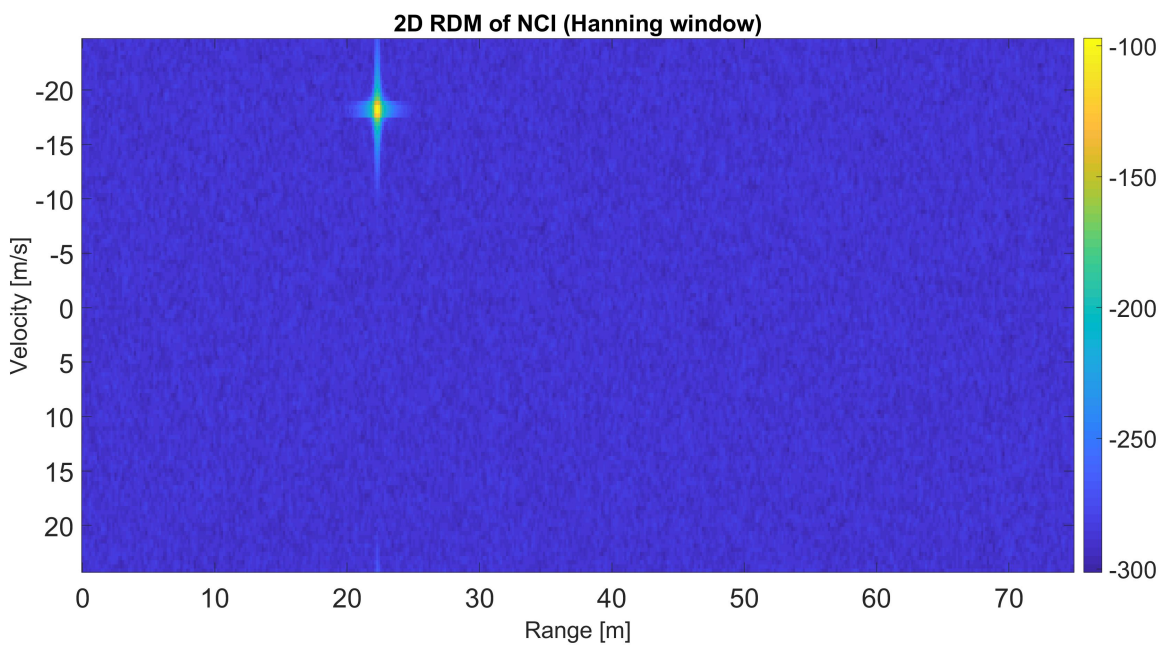


Figure 22: 2D RDM of NCI

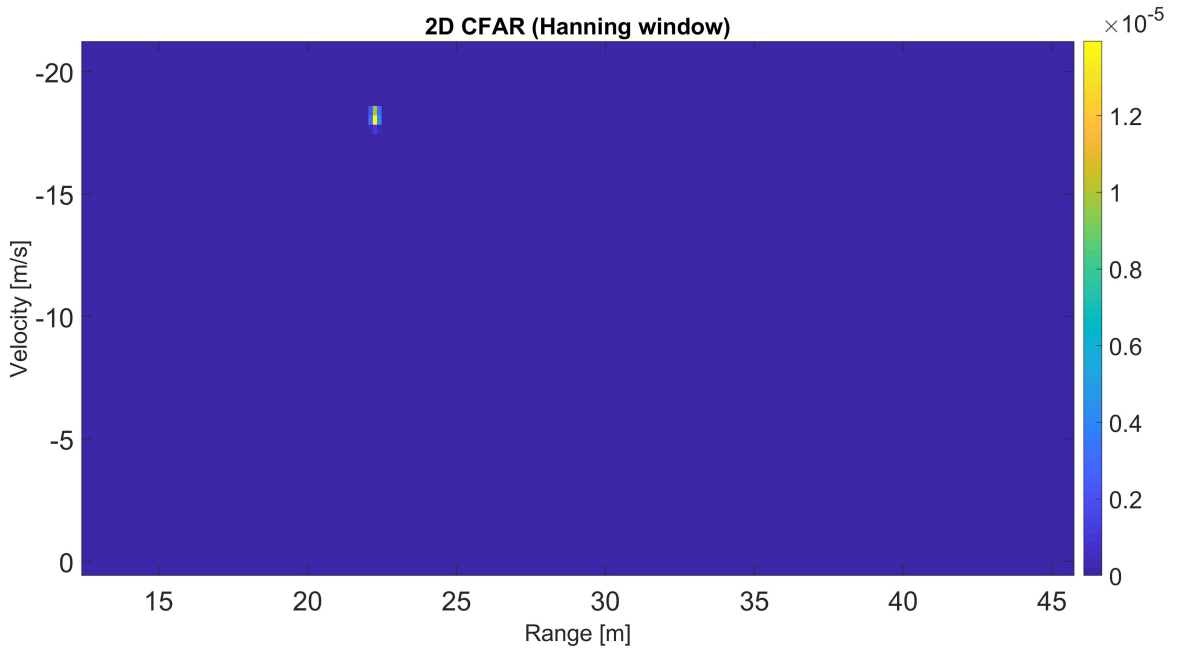


Figure 23: 2D RDM of CFAR

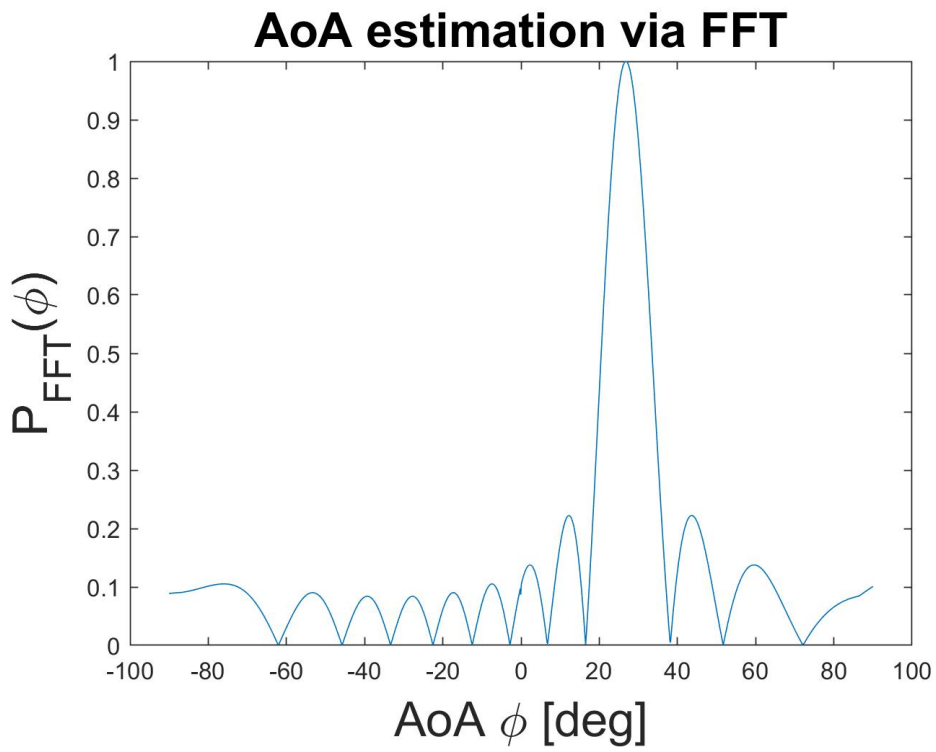


Figure 24: Angle of Arrival estimation



FMU 'HadFunction': FMI: doCalc function was called..  
 FMU 'HadFunction': FMI: The time to collision ( $T_{tc}$ ) = 2.903439  
 FMU 'HadFunction': FMI: Pedal position = 0.000000

FMU 'RadarModel': FMI: doCalc function was called..  
 FMU 'RadarModel': FMI: Estimated distance ( $R_e$ ) = 64.994068  
 FMU 'RadarModel': FMI: Virtual ground truth distance ( $R_{GT}$ ) = 65.019783

FMU 'RadarModel': FMI: Estimated velocity ( $v_e$ ) = -22.385198  
 FMU 'RadarModel': FMI: Virtual ground truth velocity ( $v_{GT}$ ) = -22.244413

Figure 25: Radar behavioral model and HAD Function FMUs output after 6.0 [s]



FMU 'HadFunction': FMI: doCalc function was called..  
 FMU 'HadFunction': FMI: The time to collision ( $T_{tc}$ ) = 1.540000  
 FMU 'HadFunction': FMI: Pedal position = 1.000000

FMU 'RadarModel': FMI: doCalc function was called..  
 FMU 'RadarModel': FMI: Estimated distance ( $R_e$ ) = 19.176178  
 FMU 'RadarModel': FMI: Virtual ground truth distance ( $R_{GT}$ ) = 19.281807

FMU 'RadarModel': FMI: Estimated velocity ( $v_e$ ) = -12.452063  
 FMU 'RadarModel': FMI: Virtual ground truth velocity ( $v_{GT}$ ) = -12.371009

Figure 26: Radar behavioral model and HADFunction FMUs output after 8.35 [s]



```

FMU 'HadFunction': FMI: doCalc function was called..
FMU 'HadFunction': FMI: The time to collision (T_tc) = 0.000000
FMU 'HadFunction': FMI: Pedal position = 1.000000

FMU 'RadarModel': FMI: doCalc function was called..
FMU 'RadarModel': FMI: Estimated distance (R_e) = 1.100428
FMU 'RadarModel': FMI: Virtual ground truth distance (R_GT) = 1.101116

FMU 'RadarModel': FMI: Estimated velocity (v_e) = 0.000000
FMU 'RadarModel': FMI: Virtual ground truth velocity (v_GT) = 0.000393

```

Figure 27: Radar behavioral model and HAD Function FMUs output after 10.53 [s]

The results shows the IF sampling approach is only feasible approach for the implementation of MIMO radar behavioral model model especially for large bandwidths like 1-4 GHz due to computation and memory issues of operating systems. FMI and OSI standards provides the opportunity to vary the radar behavioral model different parameters and CarMaker IPG control and IPG movie window is used to visualized the impact of these changes on the performance of this model.

## XI. Outlook

In order to verify the results of this radar behavioral model, further received power, magnitude and signal to noise ratio (SNR) over the distance , 2-way beam pattern of virtual antenna array in azimuth and elevation direction, maximum velocity unambiguous range, maximum angular unambiguous range, range resolution, velocity and angular resolution will be calculated respectively for further investigation in the next phase of project.

## References

- [1] J. Akesson, W. Braun, P. Lindholm, B. Bachmann *Generation of Sparse Jacobians for the Function Mock-Up Interface 2.0*. September 05, 2012.
- [2] FMI development group, *Functional Mock-up Interface for Model Exchange and Co-Simulation*. July 25, 2014.
- [3] Torsten Blochwitz, Martin Otter *Functional Mockup Interface 2.0*. September, 2012.
- [4] Torsten Blochwitz, Martin Otter *The Functional Mockup Interface for Tool independent Exchange of Simulation Models*. March 22, 2011.
- [5] Microsoft, *DLLs in Visual C++*. Internet: <https://docs.microsoft.com/en-us/cpp/build/dlls-in-visual-cpp?view=vs-2017>. January 18, 2019.
- [6] IPG Automotive, *Quick Start Guide Version 6.0.3*. 2017.

- [7] IPG Automotive, *Programmer's Guide Version 6.0.3*. 2017.
- [8] T. Hanke, N. Hirsenkorn, C. van-Driesten, P. Garcia-Ramos, M. Schiementz, S. Schneider, E. Biebl; *A generic interface for the environment perception of automated driving functions in virtual scenarios*. Internet: <https://www.hot.ei.tum.de/forschung/automotive-veroeffentlichungen>. January 22, 2019.
- [9] BMW Group; *Open Simulation Interface - Introduction and Overview*. 2017.
- [10] GitHub, *open-simulation-interface wiki*. Internet: <https://github.com/OpenSimulationInterface/open-simulation-interface/wiki>. January 21, 2019.
- [11] Open Simulation Interface 2.2.0 HTML documentation, *Open Simulation Interface 2.2.0*. January 23, 2019.
- [12] GitHub, *osi-sensor-model-packaging*. Internet: <https://github.com/OpenSimulationInterface/osi-sensor-model-packaging>. January 21, 2019.
- [13] Microsoft, *CMake support in Visual Studio*. Internet: <https://blogs.msdn.microsoft.com/vcblog/2016/10/05/cmake-support-in-visual-studio/>. January 23, 2019.
- [14] CMake, *CMake Version 3.12 Documentation*. Internet: <https://cmake.org/cmake/help/v3.12>. January 23, 2019.
- [15] Aue, R., *Sensorik : Radartechnik University of Applied Sciences Kempten*. Script for the lecture. Semester 2017/18.
- [16] Stefan Scheiblhofer, Johannes Kepler University, Linz; *A short Introduction to Range-Doppler Processing*. December 05, 2010.
- [17] W. Christian, *Radar Basics Waves and Frequency Ranges* Internet: <http://www.radartutorial.eu/02.basics/Pulse%20Radar.en.html>. December 01, 2018.
- [18] M. A. Richards., *FMCW Signals for Radar Imaging and Channel Sounding, Durham theses, Durham University*. 2015.
- [19] D.E. Barrick, *FM/CW radar signals and digital processing (No. NOAA-TR-ERL-283-WPL-26). NATIONAL OCEANIC AND ATMOSPHERIC ADMINISTRATION BOULDER CO WAVE PROPAGATION LAB*. 1973.
- [20] S.Brükel., *Script of Digital Signal Processing University of Applied Sciences Kempten* 2019.
- [21] Meinel, F., Schubert, E., Kunert, M. and Blume, H., *Real-Time Data Preprocessing for High-Resolution MIMO Radar Sensors. Towards a Common Software/Hardware Methodology for Future Advanced Driver Assistance Systems, p.133*. 2017.
- [22] Yang, C., Miller, M., Nguyen, T. and Blasch, E., *Comparative Study of Coherent, Non-Coherent, and Semi-Coherent Integration Schemes for GNSS Receivers (Preprint). SIGTEM TECHNOLOGIES INC SAN MATEO CA*. 2007.
- [23] Barkat, M. and Varshney, P.K., *On Adaptive Cell-Averaging CFAR (Constant False-Alarm Rate) Radar Signal Detection. SYRACUSE UNIV NY DEPT OF ELECTRICAL AND COMPUTER ENGINEERING*. 1987.
- [24] Schoor, M. and Yang, B., *High-resolution angle estimation for an automotive FMCW radar sensor. In Proc. Intern. Radar Symposium (IRS)*. 2007.
- [25] IPG Automotive, *Reference Manual Version 6.0.6*. 2017.